Article

Synthesis of Hyperbranched Glycoconjugates by the Combined Action of Potato Phosphorylase and Glycogen Branching Enzyme from *Deinococcus geothermalis*

Jeroen van der Vlist, Martin Faber, Lizette Loen, Teunis J. Dijkman, Lia A.T.W. Asri and Katja Loos *

Department of Polymer Chemistry & Zernike Institute for Advanced Materials, University of Groningen, Nijenborgh 4, 9747AG Groningen, The Netherlands;
E-Mails: jeroenvandervlist@gmail.com (J.V.); M.G.Faber@rug.nl (M.F.); LLoen@gmx.net (L.L.); TJDijkman@gmail.com (T.D.); L.A.T.W.Asri@rug.nl (L.A.)

* Author to whom correspondence should be addressed; E-Mail: k.u.loos@rug.nl;
Tel.: +31-50-363-6867; Fax: +31-50-363-4400.

Abstract: Potato phosphorylase is able to synthesize linear polyglucans from maltoheptaose primers. By coupling maltoheptaose to butane diamine, tris(2-aminoethyl)amine and amine functionalized amine functionalized poly ethyleneglycol (PEG), new primer molecules became available. The resulting di-, tri- and macro-primers were incubated with potato phosphorylase and glycogen branching enzyme from *Deinococcus geothermalis*. Due to the action of both enzymes, hyperbranched polyglucan arms were grown from the maltoheptaose derivatives with a maximum degree of branching of 11%. The size of the synthesized hyperbranched polyglucans could be controlled by the ratio monomer over primer. About 60%–80% of the monomers were incorporated in the glycoconjugates. The resulting hyperbranched glycoconjugates were subjected to Dynamic Light Scattering (DLS) measurements in order to determine the hydrodynamic radius and it became obvious that the structures formed agglomerates in the range of 14–32 nm.

Keywords: glycoconjugates; biohybrids; glycosyltransferases; branching enzyme; potato phosphorylase; hyperbranched; enzymatic polymerization

1. Introduction

Polysaccharides and polysaccharide conjugates are of potential interest for use in different fields of industry. The biocompatible and/or biodegradable character of polysaccharides makes them, for example, excellent candidates for use in biomedical applications [1–5]. Moreover, the renewable character of polysaccharide based polymers makes them suitable to replace olefin based polymers, for instance in the coating technology. Polysaccharides exist in nature in a variety of forms and fulfill different functions. By combining these versatile biopolymers with synthetic substrates, new functional materials may be developed.
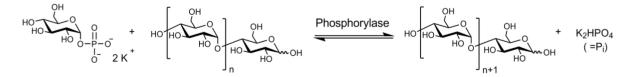
Polysaccharides are constructed *in vivo* via enzyme catalyzed reaction paths. Conventional chemical synthetic approaches are, in many cases, inadequate to provide substantial quantities of saccharides. The difficulties arise from realizing complete regio and stereo-control of the glycosylating process. At present, no such methods are available because, in chemical synthesis, most of the difficulties arise from the laborious regio- and stereochemical control. Most synthetic approaches are therefore based on the modification or degradation of naturally occurring polysaccharides resulting in less than perfect products.

In vitro enzymatic polymerizations [6–11] are superior alternatives for glycoside and saccharide synthesis as no selective protection/deprotection steps are necessary and control of configuration at newly formed anomeric centers is absolute [12,13].

Here, members from the glycosyltransferase family were used to construct biohybrid materials based on hyperbranched polysaccharides and different synthetic substrates. Potato phosphorylase (PP) and the microbial *Deinococcus geothermalis* branching enzyme (GBE$_{Dg}$) were used to construct a hyperbranched polyglucan consisting of α(1→4) linked glucose residues with defined α(1→6) linkage branches. The combined catalysis of hyperbranched polysaccharides was performed previously in solution and yielded polysaccharides with a predefined molecular weight and a degree of branching of 11% [14–17].

Potato phosphorylase (PP) catalyzed the formation of linear amylose chains (see Figure 1). Glucose-1-phosphate (G1P) acted in this reaction as donor substrate [18,19] while the acceptor substrate function was fulfilled by (multi functional) maltoheptaose adducts.
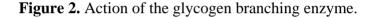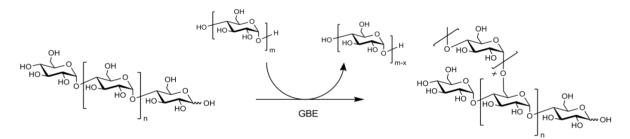
Figure 1. Action of potato phosphorylase.

The presence of an acceptor substrate (or primer) is essential for PP and makes this enzyme ideal for the preparation of bioconjugates as the primer can be chemically bound to the synthetic polymer or substrate of choice. Via this concept, amylose-like polymer chains were already grown from: Si surface [20], polystyrene [21,22], PEG [2] and Si particles [23]. The inspiring work of Pfannemüller resulted in a series of (multi)functional primers and diblock copolymers that were subsequently used as

acceptor substrate for PP [24–27]. Next to amylose, block copolymers consisting of a dextran [28–31] and hyaluronan [32,33] moiety are reported as well.

The use of a glyco moiety as a part of a diblock copolymer can result in an amphiphilic system with interesting aggregation behavior. For example, polystyrene-block-amylose (or dextran) amphiphiles can aggregate in micelles, polymersomes or vesicles [30,34–37].

However, hyperbranched polysaccharides can be realized as well with the introduction of a branching enzyme [38]. Here we use the glycogen branching enzyme of the micro-organism *Deinococcus geothermalis* (GBE$_{Dg}$) together with PP to prepare hyperbranched glycoconjugates. The branching enzyme catalyses the hydrolytic cleavage of an α(1→4) glycosidic linkage and subsequent inter- or intra-chain transfer of the non-reducing terminal fragment to the C6 hydroxyl position of an α-glucan (see Figure 2). In this process an additional non-reducing end is created which can act as primer site for PP.

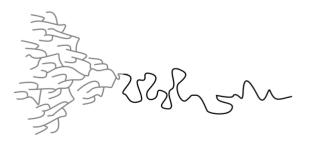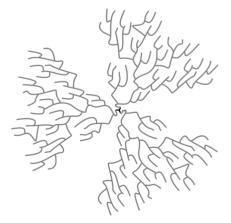**Figure 2.** Action of the glycogen branching enzyme.

PP as well as GBE$_{Dg}$ are active in the same temperature and pH range which make it possible to grow hyperbranched polyglucans from (modified) primers.

Here, primer derivatives were prepared by coupling maltoheptaose to different amine carrying molecules. Coupling took place via a reductive amination and resulted in di-functional and tri-functional primers as well as PEG macroprimers. With this it become possible to synthesize well defined synthetic hyperbranched glycoconjugates as schematically depicted in Figure 3.

Figure 3. Schematic representation of the products after the enzyme catalyzed tandem polymerization in which a hyperbranched polyglucan is grown from (**left**) amine functionalized poly ethyleneglycol (PEG) macro primer. (**right**) tri-functional primer derivative, tris(2-aminoethyl)amine (TREN)-(G7)$_3$.

The advantages of such hyperbranched polyglucan biohybrids are multiple and cover a range of potential applications. For example, glycogen, the energy storage polymer of mammals, is a hyperbranched glycoconjugate itself as it is *in vivo* grown from a central core protein known as glycogenin [39–41]. The *in vitro* approach as described in this paper to design synthetic hyperbranched glycoconjugates, may be a valuable tool in order to completely understand the biosynthesis of glycogen and its aggregation behavior. Moreover, hyperbranched glycoconjugates can be used to understand biological processes such as the multivalent or cluster effect on carbohydrate-protein interactions [5,42]. Furthermore, the abundant amount of functional end-groups at the periphery of hyperbranched polyglucans can for example be used for post-polymerization reactions or to interact with their surroundings. This makes hyperbranched glyco-based structures candidates for drug carrier purposes, as drugs can be chemically linked to the hydroxy moiety of the glucose residues or physically trapped inside the hyperbranched structure.

2. Experimental Section

2.1. Materials

Butanediamine (BDA, Aldrich) was purified by sublimation before use and tris(2-aminoethyl)amine (TREN, Aldrich) was purified via Kugelrohr distillation before use. The column material Amberlite IR-120 (H^+) ion exchange resin was purchased from Aldrich. Dimethyl sulphoxide (DMSO, Labscan) was distilled from CaH_2 prior to use. Products were dialyzed using dialysis tubing from Spectra/Por (MWCO 1000). Poly(ethylene glycol) methyl ether (PEG-OH; MW 2000 g·mol^{-1}, Aldrich) and PEG-NH$_2$ (MW 20000, Iris Biotech) were dried over P_2O_5 *in vacuo* before use. Phthalimide, triphenylphosphine (Ph$_3$P), diisopropylazodicarboxylate (DIAD), hydrazine monohydrate, sodiumcyanoborohydride and Amberlite IR-120 H^+ ion exchange resin were used as received (Aldrich).

2.2. Methods

2.2.1. Dynamic Light Scattering (DLS)

DLS measurements were performed on an ALV CGS-3 goniometer equipped with an ALV LSE-5005 multiple τ digital correlator at angles of between 30 ° and 150 ° with a 10 ° interval at room temperature. Measurements were performed in triplicate and averaged values are displayed. Fitting of the autocorrelation function was performed with the CONTIN algorithm. All samples were dissolved in water R.O. (1 mg·mL^{-1}) and filtered (0.45 μm teflon filter).

2.2.2. Elemental Analysis

Elemental analysis was performed on an EA3000 from EuroVector.

2.2.3. ^{1}H-NMR Spectroscopy

^{1}H-NMR spectra were recorded in D$_2$O on a Varian VXR spectrometer operating at 300 or 400 MHz at ambient temperatures. ^{1}H-NMR spectra used for the determination of the degree of branching were recorded on a Varian Inova 500 MHz spectrometer at 50 ℃ with pre-saturation of the

HOD resonance. 2,2-dimethyl-2-silapentane-5-sulfonic acid (DSS) was used as an external reference. Complete relaxation of the protons was ensured by taking a 10 s pause between pulses.

2.2.4. ATR Infra-Red Spectroscopy

Attenuated total reflection fourier transform infra-red (ATR FT-IR) spectra were recorded on a Bruker IFS88 spectrometer equipped with a MCT-A detector at a resolution of 4 cm^{-1} using an average of 50 scans for sample and reference.

2.3. Isolation and Purification of the Glycosyltransferases

Phosphorylase was isolated from potatoes via an ammonium sulfate precipitation procedure in which the phosphorylase was selectively precipitated and resuspended in a citric acid buffer. α-Amylase was removed via a heat treatment of the suspension. The phosphorylase suspension was eventually dialyzed and concentrated and stored at 4 °C. A more elaborate procedure of the isolation and the purification of potato phosphorylase [14] is described elsewhere. The cloning, expression and purification of the GBE$_{Dg}$ is reported elsewhere [43].

2.4. Synthesis of Maltoheptaose

Maltoheptaose was obtained after the acid catalyzed hydrolysis of β-cyclodextrin in a yield of 10%. Residual β-cyclodextrin was removed as a p-xylene/ β-cyclodextrin complex. A more elaborate procedure is described elsewhere [14].

2.5. Synthesis of Primer Adducts

2.5.1. Di-Functional Primer Adduct, BDA-(G7)$_2$

BDA (100 mg, 1 mol eq.), maltoheptaose (1.31 g, 1 mol eq.) and NaCNBH$_3$ (107 mg, 1.5 mol eq.) were dissolved in 6 mL DMSO containing 1 V/V% acetic acid and 3 Å molsieves. This mixture was placed in an incubator at 65 °C and was shaken for 6 days. After 3 days 1.5 mol eq. NaCNBH$_3$ and 0.9 mol eq. maltoheptaose were added. The reaction mixture was precipitated in ethanol, filtrated over a p4 glass filter, washed with acetone and ethanol and dried *in vacuo*, yielding a yellow powder (2.77 g). The product was dissolved in 50 mL water containing Amberlite IR-120 (H$^+$) beads and was shaken overnight in an incubator at 40 °C. The solution was lyophilized yielding a yellow powder (1.69 g/61%).

^{1}H-NMR (D$_2$O, 300 MHz). 5.39 ppm: H1(m) and H1(n) of glucose residue, 5.11 ppm: CH$_2$-NH, 4.12–3.51 ppm: glucose residue, 3.41 ppm: H4(m).

FT-IR. OH stretching glucose residues: 3683–2991 cm^{-1}, CH and CH$_2$ stretching: 2923 cm^{-1}, water deformation band: 1640 cm^{-1}, OH: 1358 cm^{-1}

2.5.2. Synthesis of Tri-Functional Primer Adduct, TREN-(G7)$_3$

TREN (100 μL, 1 mol eq.), maltoheptaose (1.16 g, 1.5 mol eq.) and NaCNBH$_3$ (126 mg, 3 mol eq.) were dissolved in 6 mL DMSO containing 1 V/V% acetic acid and 3 Å molsieves. This mixture was placed in an incubator at 65 ℃ and was shaken for 6 days. 1.5 mol eq. NaCNBH$_3$ and 1.4 mol eq. maltoheptaose were added after 3 days. The reaction mixture was precipitated in ethanol, filtrated over a p4 glass filter, washed with acetone and ethanol and dried *in vacuo*, yielding a yellow powder (2.26 g). The product was dissolved in 50 mL water containing Amberlite IR-120 (H$^+$) beads and was shaken over night in an incubator at 40 ℃. The solution was lyophilized yielding a yellow powder (1.01 g/45%).

^{1}H-NMR (D$_2$O, 300 MHz). 5.39 ppm: H1(m) and H1(n) of glucose residue, 5.11 ppm: CH$_2$-NH, 4.12–3.51 ppm: glucose residue, 3.41 ppm: H4(m).

ATR FT-IR. OH stretching glucose residues: 3683–2991 cm^{-1}, CH and CH$_2$ stretching: 2923 cm^{-1}, water deformation band: 1640 cm^{-1}, OH: 1358 cm^{-1}

2.5.3. Synthesis of PEG Phthalimide Intermediate (Mitsunobu)

PEG-OH (5 g, 2.5 mmol, MW 2,000 g·mol^{-1}), triphenylphosphine (0.62 g, 10 mmol), phthalimide (1.47 g, 10 mmol) and THF (50 mL) were mixed in a round-bottomed flask equipped with a magnetic stirrer at 0 ℃ under a N$_2$ atmosphere. To this mixture diisopropyl azodicarboxylate (1.9 mL, 10 mmol) was added drop wise. After the addition, the temperature was raised to 25 ℃ and the reaction mixture was allowed to stir for 24 h. Ethanol (200 mL) was added and the reaction mixture was stirred for another 30 minutes. The solvent was evaporated by means of rotation evaporation and the resulting PEG-phthalimide was dissolved in water. The excess starting material was extracted with 3 portions of diethyl ether and discarded. Finally, the product was lyophilized, yielding a white powder (4.7 g, 94%).

^{1}H-NMR (d-DMSO, 300 MHz): 7.8 ppm: benzylic protons endgroup, 3.7 ppm: CH$_2$-phtalimide, 3.5 ppm: O-CH$_2$ PEG backbone, 3.2 ppm: CH$_3$ endgroup.

ATR FT-IR: 2880 cm^{-1}: C-H stretching, 1712 cm^{-1}: C=O stretching, 1396 cm^{-1}: C-N stretching, 1100 cm^{-1}: C-O stretching (PEG backbone).

2.5.4. Synthesis of PEG-NH$_2$ (Hydrazynolysis)

4.7 g PEG-phthalimide and hydrazine monohydrate (5 mL) were added to ethanol (40 mL) in a round-bottomed flask equipped with a magnetic stirrer. The mixture was refluxed for 24 h and the solvent was removed via rotation evaporation. The remaining product was dissolved in CH$_2$Cl$_2$ (100 mL) and the precipitated by-products were removed by filtration. The filtrate was precipitated in diethyl ether and dried *in vacuo*, yielding an off-white powder (3.7 g, 78%).

^{1}H-NMR (d-DMSO, 300 MHz): 3.7 ppm: CH$_2$-NH$_2$, 3.5 ppm: O-CH$_2$ PEG backbone, 3.2 ppm: CH$_3$ end-group, 2.6 CH$_2$-NH$_2$.

ATR FTIR: 2880 cm^{-1}: C-H stretching, 2327 cm^{-1}: NH$_3^+$ salt, 1665 cm^{-1}: phthalhydrazide impurity, 1582 cm^{-1}: N-H bending (primary amine), 1100 cm^{-1}: C-O stretching (PEG backbone).

2.5.5. Synthesis of PEG Macro Primer Adduct, PEG-(G7)$_1$

PEG-NH$_2$ (0.29 g, 0.145 mmol, 5.0 eq), Maltoheptaose (33 mg, 0.029 mmol, 1.0 eq), NaCNBH$_3$ (9 mg, 0.145 mmol, 5.0 eq) and acetic acid (8 μL, 0.145 mmol, 5.0 eq) were dissolved in 5 mL DMF containing 3 Å molsieves. This mixture was placed in an incubator at 65 ℃ and was shaken for 6 days. After 3 days NaCNBH$_3$ (10 mg) and acetic acid (10 μL) were added. The reaction mixture was precipitated in Et$_2$O, filtrated over a p4 glass filter, washed with Et$_2$O and dried *in vacuo*, yielding a white powder (145 mg). The product was dissolved in 50 mL water containing Amberlite IR-120 (H$^+$) beads and was shaken over night in an incubator at 40 ℃. The solution was lyophilized yielding a white powder (108 mg).
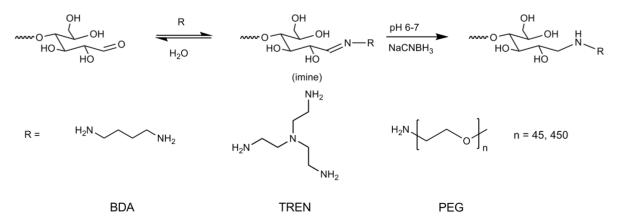
2.6. Typical Enzyme Catalyzed Polymerization

Primer (0.5 mM), G1P (25–500 mM), phosphorylase (5 U·mL^{-1}) and GBE$_{Dg}$ (250 U·mL^{-1}) were mixed and filled to 5 mL MOPS buffer (pH 7.0, 50 mM). When only phosphorylase was utilized a citrate buffer (pH 6.2, 50mM) was used. Different ratios G1P to primer were used by varying the G1P concentration. The solution was depending on the enzymes used incubated at 37 ℃ (tandem polymerization) or 38 ℃ (phosphorylase) in a shaking incubator. The released amount of phosphate was measured with a modified [44] method of Fiske and Subbarow [45]. Upon reaching equilibrium conditions the reaction was stopped by a heat treatment (5 min in boiling water). Denaturated enzymes were removed by means of centrifugation. Dialysis (MWCO 1000) and lyophilization of the remaining solution yields the hyperbranched bioconjugates.

3. Results and Discussion

3.1. Synthesis and Purification of Primer Adducts

In order to prepare difunctional-, trifunctional- and macro- primers, maltoheptaose was respectively coupled to butane diamine (BDA), tris(2-aminoethyl)amine (TREN) and amine functionalized methyl-ether-polyethylene glycol (PEG) with a molecular weight of 2000 g·mol^{-1} (PEG$_{45}$) and 20,000 g·mol^{-1} (PEG$_{454}$).

Figure 4. General reaction mechanism of a reductive amination with the reducing group of a saccharide.

Coupling took place via a reductive amination with NaCNBH$_3$ as reducing agent (see Figure 4). The reducing group of the maltoheptaose reacts herein with the primary amines of the amine functionalized core molecules and the formed imine intermediate was subsequently reduced to a secondary amine [46–48].

Hydroxyl-PEG$_{454}$ methylether was first converted via a Mitsunobu hydrazinolysis to an amine functionalized PEG methylether [49,50], while PEG$_{45}$ was directly bought as an amine functionalized PEG.

Coupling of the maltoheptaose was done with a small excess of amine groups. This reaction pathway resulted in a mixture of complete primer functionalized core molecules [represented as BDA-(G7)$_2$, TREN-(G7)$_3$ and PEG-(G7)] and partly functionalized core molecules, having one or more unreacted amine groups [BDA-(G7)$_1$, TREN-(G7)$_1$, TREN-(G7)$_2$ and PEG-NH$_2$] and is presented in Figure 5.
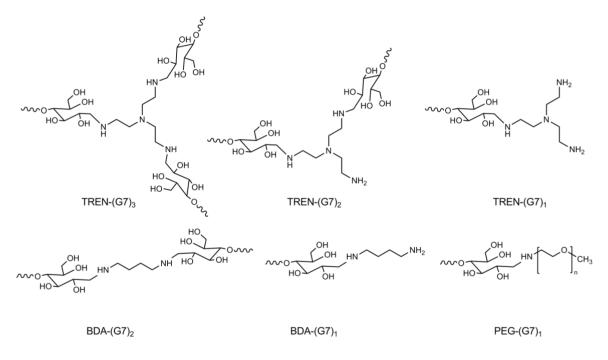
Figure 5. The different reaction products after reductive amination.

Purification of the above described mixture was possible with Amberlite IR-120 (H$^+$) resin. This strong cation-exchange resin was able to adsorb amine functionalized molecules [51,52]. The unreacted and partly reacted core molecules could therefore be separated from the product in a yield of 45% to 61%. Eventually, the adsorbed side products could be isolated for evaluation purposes. This was done by exposing the Amberlite beads to a 10% ammonia solution. The amine containing side products were with this treatment released and isolated by means of lyophilization.

The carbon, hydrogen and nitrogen content of the water eluted and ammonia eluted fractions were determined with elemental analysis and are listed in Table 1. Especially the nitrogen content is a good measure to distinct the fully substituted products from the partly substituted products. The nitrogen content of BDA-(G7)$_1$ is 1.9 times higher than BDA-(G7)$_2$. The nitrogen content of TREN-(G7)$_1$ and TREN-(G7)$_2$ is respectively 2.77 and 1.46 times higher when compared to the nitrogen content of TREN-(G7)$_3$. This quantitative difference in nitrogen content is a clear indication of a successful purification. Unfortunately, this method could not be used for the PEG adducts since the elemental
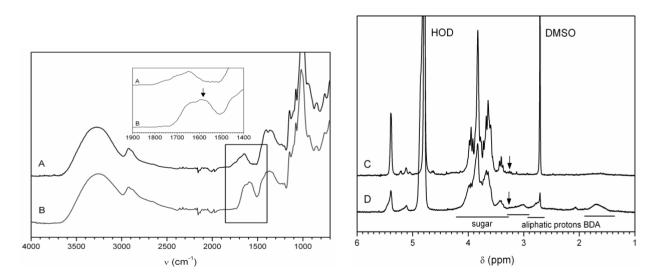
composition of PEG-NH$_2$ and PEG-(G7)$_1$ do not differ enough to discriminate on the basis of the nitrogen content.

Table 1. Elemental analysis results after purification with Amberlite IR-120 (H$^+$).

Compound	Eluted with	Theoretical (%)			Observed (%)		
		C	H	N	C	H	N
BDA-(G7)$_2$	Water	44.74	6.66	*1.19*	39.67	5.98	*1.23*
BDA-(G7)	10% ammonia	45.10	6.91	*2.29*	40.79	6.35	*3.67*
TREN-(G7)$_3$	Water	44.57	6.63	*1.58*	38.96	6.06	*1.69*
TREN-(G7)$_2$,	} 10% ammonia	44.66	6.75	*2.31*	38.82	6.36	*3.05*
TREN-(G7)		44.93	7.07	*4.37*			

Furthermore, ATR-FTIR and ^{1}H-NMR analyses confirmed the successful syntheses and purification of the different (multi)functional primers, see Figure 6. The N-H bending vibration of (unreacted) primary amines at a wave number of 1593 cm^{-1} were no longer detectable via ATR-FTIR while the isolated side products do still show a clear signal at 1593 cm^{-1}. Moreover, the H2β signal of maltoheptaose, which is normally present at 3.26 ppm, could not be detected by ^{1}H-NMR which is an indication of a successful coupling as well. It has to be noted that the aliphatic protons of the core molecules were not visible in the NMR spectrum. It is assumed that aggregate formation shielded the protons in the core molecule.

Figure 6. (**Left**) ATR-FTIR spectra of (**A**) butane diamine (BDA)-(G7)$_2$ and (**B**) BDA-(G7)$_1$. (**Right**) ^{1}H-NMR spectra of (**C**) BDA-(G7)$_2$ and (**D**) BDA-(G7)$_1$.
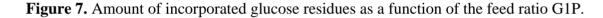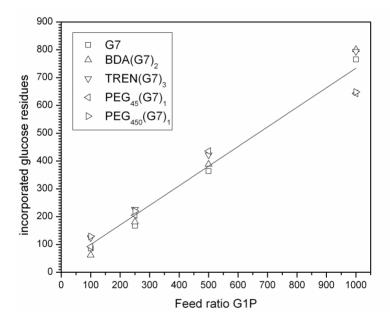

3.2. Enzyme Catalyzed Synthesis of Hyperbranched Glycoconjugates

The synthesized primer adducts were used to start an enzyme catalyzed tandem polymerization. Due to the acceptor donor specificity of PP, glucose residues were only coupled to the synthesized maltoheptaose adducts carrying 1 or more maltoheptaose residues. Phosphorylase catalyzed herein the linear growth of the polyglucan while BGE$_{Dg}$ catalyzed the branch formation. By taking different ratios of G1P to primer (represented as "feed ratio G1P" on the x-axis in Figure 7) structures with

differently sized hyperbranched polysaccharide moiety were realized. With each glucose residue added to the acceptor substrate, an inorganic phosphate is released. By measuring the amount of released inorganic phosphate via the (modified) [44] method as proposed by Fiske and Subbarow [45] it became possible to measure the amount of incorporated glucose residues.

Figure 7 shows the amount of incorporated glucose residues after 24 h of incubation with PP and GBE_{Dg}. For all modified primers a linear dependency was observed just like in controlled/living polymerizations in which the degree of polymerization is related to the ratio monomer over initiator concentration. Only for the $PEG-(G7)_1$ primed reactions, a deviation was seen at a feed ratio of 1000. These deviations may be due to the fact that equilibrium conditions were not yet reached after 24 h. The conversion of the differently primed reactions varied from 62% for $PEG-(G7)_1$ primed reactions to 80% for $TREN-(G7)_3$ primed reactions. However, in general reactions catalyzed with PP resulted in conversions between 60% and 80% and there is no evidence that the core molecules interfere with the PP catalyzed polymerization. In conclusion, by choosing the feed ratio G1P, the length of the hyperbranched polyglucan chains can be predetermined and bioconjugates can be realized with differently sized glyco moieties.

Figure 7. Amount of incorporated glucose residues as a function of the feed ratio G1P.

GBE_{Dg} catalyzed the branch formation in the tandem polymerization. Branch formation occurred only at the $\alpha(1\rightarrow4,6)$ position to an average extend of 11% in the case of maltoheptaose primed reactions as was determined with ^{1}H-NMR [53,54]. The NMR-signal (at 5.0 ppm) of the anomeric protons of the $\alpha(1\rightarrow4,6)$ linked glucose residues were used to quantify the degree of branching and is expressed as a percentage.

$$\text{Degree of branching } = \frac{H1(1,4\rightarrow6)}{H1(m) + H1(n) + H1(1,4\rightarrow6)} \cdot 100\% \tag{1}$$

H1(m) and H1(n) are the H1 protons of glucose residues in the middle of the chain and at the non-reducing end (both at 5.4 ppm) respectively. Figure 8 shows the degree of branching for a given feed ratio of G1P. The continuous curve gives the theoretical degree of branching if on average every

9th glucose residue acts as a branching point and approaches a degree of branching of 11%. Whereas the difunctional BDA-(G7)$_2$ and trifunctional bioconjugates TREN-(G7)$_3$ followed the G7 primed branching profile, the synthesized PEG diblock copolymers showed a degree of branching below average. The hydrophilic PEG chains may interfere with the branch formation resulting in a decreased branching profile. Nevertheless, a degree of branching of 8% was obtained for the hyperbranched diblock copolymers at a high feed ratio of G1P.
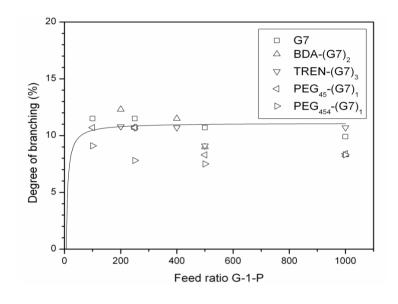
Figure 8. Degree of branching as a function of the feed ratio G1P.

3.3. Dynamic Light Scattering (DLS) Analysis of Hyperbranched Glycoconjugates

The different hyperbranched glycoconjugates were subjected to dynamic light scattering measurements in order to study the particle size. DLS measurements showed diameters in the order of 14–28 nm depending on the feed ratio G1P. The DLS autocorrelation functions of the hyperbranched glycoconjugates were recorded with DLS in triple, the CONTIN algorithm was used to calculate the decay rates (Γ) of the distribution functions at different scattering vectors (q). The translational diffusion coefficient (D_t) was obtained from the decay time (τ), according to the relationship as displayed in Equation (2).

$$\frac{1}{\tau} = \Gamma = q^2 D_t \qquad (2)$$

The diffusion coefficient is related to the hydrodynamic radius (R_H) via the Stokes-Einstein Equation (3). Since the Stokes-Einstein relation is only valid for hard spherical particles the term apparent hydrodynamic radius is introduced ($R_{H(app)}$).

$$R_{H(app)} = \frac{k_B T}{6\pi\eta D_t} \qquad (3)$$

where k_B, T and η are the Boltzmann constant, temperature (K) and the solvent viscosity.

A linear variation of Γ *versus* q^2 passing through the origin is characteristic of a translational diffusive process typical for spherical particles [55]. Although Figure 9 shows only one example

(di-functional primer, BDA-(G7)$_2$, it is representative for all measurements as conducted in this research proving that all aggregates have a spherical form.

Figure 9. (**Left**) Example of the distribution functions as calculated with CONTIN at angles between 30° and 150°. (**Right**) Example of the determination of the D$_t$ from the linear function $\Gamma(q^2)$.
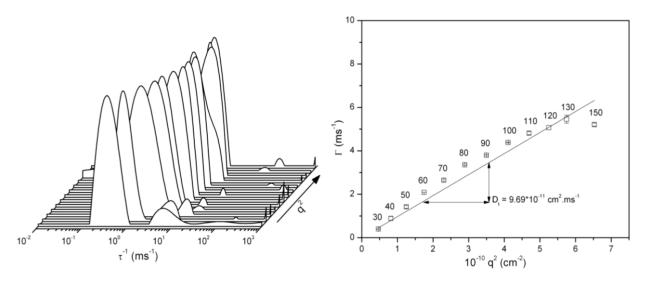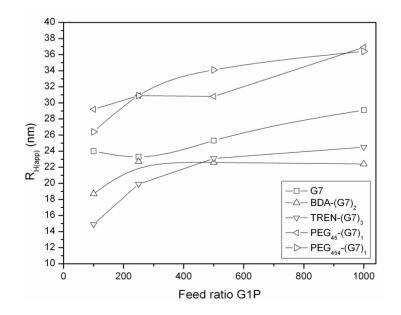

Figure 10 shows the resulting apparent hydrodynamic radii of the hyperbranched glycoconjugates. The radii increased to a certain extent with increasing feed ratio G1P. The radii of BDA-(G7)$_2$ and TREN-(G7)$_3$ based glycoconjugates level off at higher feed ratios G1P. Steric hindrance at the periphery may be responsible as this phenomenon is also seen for dendrimers at higher generations [56]. The volume required for the exponential growth of dendrimers at higher generations is not available since the volume increases only cubically. The hyperbranched glycoconjugates with BDA-(G7)$_2$ and TREN-(G7)$_3$ as core molecules can be compared with the initiator cores used in the divergent synthesis of dendrimers and the same limitation in growth is seen.

Figure 10. Relation of the apparent hydrodynamic radius with the feed ratio G1P.

The G7 primed products and the PEG based diblock copolymers do not show this plateau because the available space for chain growth is hardly limiting. Surprisingly, the two different PEG diblock copolymers cannot be distinguished by hydrodynamic radius although the molecular weight of the PEG block varies from 2000 g·mol^{-1} to 20000 g·mol^{-1}. This can be explained by the fact that the hydrodynamic volume of PEG$_{45}$ and PEG$_{454}$ in water are an order smaller than the size of the observed particles. The hydrodynamic radius of PEG$_{45}$ and PEG$_{454}$ are, respectively, ~1.3 nm and ~4.5 nm [57]. When the PEG chains are entangled (interpenetrating coils), the contribution of the PEG block to the volume increase of the glycoconjugates is negligible.

Water soluble hyperbranched polysaccharides tend to form aggregates in water due to intermolecular hydrogen bonding between the abundant hydroxy groups. Therefore, the hydrodynamic radii as shown in Figure 7 represent the radii of aggregates rather than single polymer chains. The increase in feed ratio of G-1-P therefore results in aggregates build up from larger hyperbranched polysaccharides. To obtain more information about the aggregate formation light scattering measurements should be conducted with DMSO as solvent instead of water. DMSO is known to break the inter- and intramolecular hydrogen bonds of polysaccharides, leading to the dispersion of the aggregates and making it may be possible to study individual polymer chains.

4. Conclusions

The coupling of maltoheptaose to butane diamine (BDA), tris(2-aminoethyl)amine (TREN) and amine functionalized poly ethyleneglycol (PEG) via a reductive amination resulted in 2-, 3-functional primers and, in the case of PEG, in macroprimers. Phosphorylase was able to start polymerization from these modified maltoheptaose derivatives. By combining the action of potato phosphorylase with the glycogen branching enzyme from *Deinococcus geothermalis,* hyperbranched polyglucan "arms" were grown from the modified acceptor substrates. Therefore, we have shown that with this technique it becomes possible to grow linear as well as hyperbranched polyglucans from virtually any substrate.

The degree of branching was limited to 11% due the specificity of the GBE$_{Dg}$. However, the hydrophilic PEG chains caused a decrease in branching density as the degree of branching dropped to 8% in the case of the diblock copolymers. Non-specific interaction of the PEG chains may reduce the enzyme activity. The size of the hyperbranched glyco moiety can be controlled by the feed ratio of G1P. About 60 to 80% of G1P was consumed by PP and incorporated in the hyperbranched polyglucan. DLS measurements showed the hydrodynamic radii of the different hyperbranched glycoconjugates. The measured radii are the result of aggregate formation of different hyperbranched structures.

References

1. Houga, C.; Giermanska, J.; Lecommandoux, S.; Borsali, R.; Taton, D.; Gnanou, Y.; Le Meins, J.F. Micelles and polymersomes obtained by self-assembly of dextran and polystyrene based block copolymers. *Biomacromolecules* **2009**, *10*, 32–40.

2. Akiyoshi, K.; Kohara, M.; Ito, K.; Kitamura, S.; Sunamoto, J. Enzymatic synthesis and characterization of amphiphilic block copolymers of poly(ethylene oxide) and amylose. *Macromol. Rapid Commun.* **1999**, *20*, 112–115.

3. Liu, J.Y.; Zhang, L.M. Preparation of a polysaccharide-polyester diblock copolymer and its micellar characteristics. *Carbohydr. Polym.* **2007**, *69*, 196–201.

4. Hernandez, O.S.; Soliman, G.M.; Winnik, F.M. Synthesis, reactivity, and pH-responsive assembly of new double hydrophilic block copolymers of carboxymethldextran and poly(ethylene glycol). *Polymer* **2007**, *48*, 921–930.

5. Spain, S.G.; Gibson, M.I.; Cameron, N.R. Recent advances in the synthesis of well-defined glycopolymers. *J. Polym. Sci. Part A* **2007**, *45*, 2059–2072.

6. Shoda, S.; Izumi, R.; Fujita, M. Green process in glycotechnology. *Bull. Chem. Soc. Jpn.* **2003**, *76*, 1–13.

7. Kadokawa, J. Precision polysaccharide synthesis catalyzed by enzymes. *Chem. Rev.* **2011**, *111*, 4308–4345.

8. Loos, K. *Biocatalysis in Polymer Chemistry*; Wiley: Hoboken, NJ, USA, 2010.

9. Palmans, A.R.A.; Heise, A. *Enzymatic Polymerisation*; Springer: Berlin, Germany, 2010.

10. Cheng, H.N.; Gross, R.A. *Green Polymer Chemistry: Biocatalysis and Biomaterials*; American Chemical Society: New York, NY, USA, 2010.

11. Kobayashi, S.; Makino, A. Enzymatic polymer synthesis: An opportunity for green polymer chemistry. *Chem. Rev.* **2009**, *109*, 5288–5353.

12. Van der Vlist, J.; Loos, K. Enzymatic polymerizations of polysaccharides. In *Biocatalysis in Polymer Chemistry*, 1st ed.; Loos, K., Ed.; Wiley: Hoboken, NJ, USA, 2010.

13. Van der Vlist, J.; Loos, K. Transferases in polymer chemistry. *Adv. Polym. Sci.* **2010**, *237*, 21–54.

14. Van der Vlist, J.; Reixach, M.P.; van der Maarel, M.; Dijkhuizen, L.; Schouten, A.J.; Loos, K. Synthesis of branched polyglucans by the tandem action of potato phosphorylase and deinococcus geothermalis glycogen branching enzyme. *Macromol. Rapid Commun.* **2008**, *29*, 1293–1297.

15. Ciric, J.; Loos, K. Synthesis of branched polysaccharides with tunable degree of branching. **2012**, submitted.

16. Kajiura, H.; Kakutani, R.; Akiyama, T.; Takata, H.; Kuriki, T. A novel enzymatic process for glycogen production. *Biocatal. Biotransform.* **2008**, *26*, 133–140.

17. Fujii, K.; Takata, H.; Yanase, M.; Terada, Y.; Ohdan, K.; Takaha, T.; Okada, S.; Kuriki, T. Bioengineering and application of novel glucose polymers. *Biocatal. Biotransformation* **2003**, *21*, 167–172.

18. Seibel, J.; Joerdening, H.; Buchholz, K. Glycosylation with activated sugars using glycosyltransferases and transglycosidases. *Biocatal. Biotransformation* **2006**, *24*, 311–342.

19. Kitaoka, M.; Hayashi, K. Carbohydrate-processing phosphorolytic enzymes. *Trends Glycosci. Glycotechnol.* **2002**, *14*, 35–50.

20. Van der Vlist, J.; Schonen, I.; Loos, K. Utilization of glycosyltransferases for the synthesis of a densely packed hyperbranched polysaccharide brush coating as artificial glycocalyx. *Biomacromolecules* **2011**, *12*, 3728–3732.

21. Narumi, A.; Kawasaki, K.; Kaga, H.; Satoh, T.; Sugimoto, N.; Kakuchi, T. Glycoconjugated polymer 6. Synthesis of poly[styrene-block-(styrene-*graft*-amylose) via potato phosphorylase catalyszed polymerization. *Polym. Bull.* **2003**, *49*, 405–410.

22. Loos, K.; Müller, A.H.E. New routes to the synthesis of amylose-block-polystyrene rod-coil block copolymers. *Biomacromolecules* **2002**, *3*, 368–373.

23. Loos, K.; vonBraunmühl, V.; Stadler, R.; Landfester, K.; Spiess, H.W. Saccharide modified silica particles by enzymatic grafting. *Macromol. Rapid Commun.* **1997**, *18*, 927–938.

24. Ziegast, G.; Pfannemüller, B. Linear and star-shaped hybrid polymers. 1. A new method for the conversion of hydroxyl end groups of poly(oxyethylene) and other polyols into amino end groups. *Makromol. Chem. Rapid Commun.* **1984**, *5*, 363–371.

25. Ziegast, G.; Pfannemüller, B. Linear and star-shaped hybrid polymers. 2. Coupling of monosaccharide and oligosaccharide to alpha,omega-diamino substituted poly(oxyethylene) and multifunctional amines by amide linkage. *Makromol. Chem. Rapid Commun.* **1984**, *5*, 373–379.

26. Ziegast, G.; Pfannemüller, B. Linear and star-shaped hybrid polymers. 3. An improved purification procedure for coupling products of oligosaccharides by amide linkage. *Makromol. Chem. Macromol. Chem. Phys.* **1984**, *185*, 1855–1866.

27. Ziegast, G.; Pfannemüller, B. Linear and star-shaped hybrid polymers. 4. Phosphorolytic syntheses with di-functional, oligo-functional and multifunctional primers. *Carbohydr. Res.* **1987**, *160*, 185–204.

28. Bosker, W.T.E.; Agoston, K.; Cohen Stuart, M.A.; Norde, W.; Timmermans, J.W.; Slaghek, T.M. Synthesis and interfacial behavior of polystyrene-polysaccharide diblock copolymers. *Macromolecules* **2003**, *36*, 1982–1987.

29. Houga, C.; Le Meins, J.F.; Borsali, R.; Taton, D.; Gnanou, Y. Synthesis of ATRP-induced dextran-b-polystyrene diblock copolymers and preliminary investigation of their self-assembly in water. *Chem. Commun.* **2007**, 3063–3065.

30. Hernandez, O.S.; Soliman, G.M.; Winnik, F.M. Synthesis, reactivity, and pH-responsive assembly of new double hydrophilic block copolymers of carboxymethyldextran and poly(ethylene glycol). *Polymer* **2007**, *48*, 921–930.

31. Schatz, C.; Louguet, S.; le Meins, J.F.; Lecommandoux, S. Polysaccharide-block-polypeptide copolymer vesicles: Towards synthetic viral capsids. *Angew. Chem. Int. Ed.* **2009**, *48*, 2572–2575.

32. Upadhyay, K.K.; le Meins, J.F.; Misra, A.; Voisin, P.; Bouchaud, V.; Ibarboure, E.; Schatz, C.; Lecommandoux, S. Biomimetic doxorubicin loaded polymersomes from hyaluronan-block-poly(gamma-benzyl glutamate) copolymers. *Biomacromolecules* **2009**, *10*, 2802–2808.

33. Yang, Y.L.; Kataoka, K.; Winnik, F.M. Synthesis of diblock copolymers consisting of hyaluronan and poly(2-ethyl-2-oxazoline). *Macromolecules* **2005**, *38*, 2043–2046.

34. Loos, K.; Böker, A.; Zettl, H.; Zhang, A.F.; Krausch, G.; Müller, A.H.E. Micellar aggregates of amylose-block-polystyrene rod-coil block copolymers in water and THF. *Macromolecules* **2005**, *38*, 873–879.

35. Soliman, G.M.; Winnik, F.M. Enhancement of hydrophilic drug loading and release characteristics through micellization with new carboxymethyldextran-PEG block copolymers of tunable charge density. *Int. J. Pharm.* **2008**, *356*, 248–258.

36. Akiyoshi, K.; Maruichi, N.; Kohara, M.; Kitamura, S. Amphiphilic block copolymer with a molecular recognition site: Induction of a novel binding characteristic of amylose by self-assembly of poly(ethylene oxide)-block-amylose in chloroform. *Biomacromolecules* **2002**, *3*, 280–283.

37. Houga, C.; Giermanska, J.; Lecommandoux, S.; Borsali, R.; Taton, D.; Gnanou, Y.; le Meins, J. Micelles and polymersomes obtained by self-assembly of dextran and polystyrene based block copolymers. *Biomacromolecules* **2009**, *10*, 32–40.

38. Palomo, M.; Pijning, T.; Booiman, T.; Dobruchowska, J.M.; van der Vlist, J.; Kralj, S.; Planas, A.; Loos, K.; Kamerling, J.P.; Dijkstra, B.W.; *et al.* Thermus thermophilus glycoside hydrolase family 57 branching enzyme crystal structure, mechanism of action and products formed. *J. Biol. Chem.* **2011**, *286*, 3520–3530.

39. Geddes, R.; Harvey, J.D.; Wills, P.R. Molecular-size and shape of liver-glycogen. *Biochem. J.* **1977**, *163*, 201–209.

40. Geddes, R. Glycogen: A metabolic viewpoint. *Biosci. Rep.* **1986**, *6*, 415–428.

41. Smythe, C.; Cohen, P. The discovery of glycogenin and the priming mechanism for glycogen biogenesis. *Eur. J. Biochem.* **1991**, *200*, 625–631.

42. Miura, Y. Synthesis and biological application of glycopolymers. *J. Polym. Sci. Part A* **2007**, *45*, 5031–5036.

43. Palomo, R.M.; Kralj, S.; van der Maarel, M.J.E.C.; Dijkhuizen, L. The unique branching patterns of *deinococcus* glycogen branching enzymes are determined by their N-termnal domains. *Appl. Environ. Microbiol.* **2009**, *75*, 1355–1362.

44. Lowry, O.H.; Lopez, J.A. The Determination of inorganic phosphate in the presence of labile phosphate esters. *J. Biol. Chem.* **1946**, *162*, 421–428.

45. Fiske, C.H.; Subbarow, Y. The colorimetric determination of phosphorus. *J. Biol. Chem.* **1925**, *66*, 375–400.

46. Lane, C.F. Sodium cyanoborohydride—Highly selective reducing agent for organic functional groups. *Synth. Stuttg.* **1975**, 135–146.

47. Borch, R.F.; Bernstei, M.D.; Durst, H.D. Cyanohydridoborate anion as a selective reducing agent. *J. Am. Chem. Soc.* **1971**, *93*, 2897–2904.

48. Yalpani, M.; Brooks, D.E. Selective chemical modifications of dextran. *J. Polym. Sci. Part A* **1985**, *23*, 1395–1405.

49. Ryoo, S.J.; Kim, J.; Kim, J.S.; Lee, Y.S. Efficient methods of converting hydroxyl groups into amino groups in poly(ethylene glycol)-grafted polystyrene resin. *J. Comb. Chem.* **2002**, *4*, 187–190.

50. Mitsunobu, O. The use of diethyl azodicarboxylate and triphenylphosphine in synthesis and transformation of natural-products. *Synth. Stuttg.* **1981**, 1–28.

51. Sisu, E.; Bosker, W.T.E.; Norde, W.; Slaghek, T.M.; Timmermans, J.W.; Peter-Katalinic, J.; Cohen-Stuart, M.A.; Zamfir, A.D. Electrospray ionization quadrupole time-of-flight tandem mass spectrometric analysis of hexamethylenediamine-modified maltodextrin and dextran. *Rapid Commun. Mass Spectrom.* **2006**, *20*, 209–218.

52. Perdivara, I.; Sisu, E.; Sisu, I.; Dinca, N.; Tomer, K.B.; Przybylski, M.; Zamfir, A.D. Enhanced electrospray ionization fourier transform ion cyclotron resonance mass spectrometry of long-chain polysaccharides. *Rapid Commun. Mass Spectrom.* **2008**, *22*, 773–782.

53. Mcintyre, D.D.; Ho, C.; Vogel, H.J. One-dimensional nuclear-magnetic-resonance studies of starch and starch products. *Starch* **1990**, *42*, 260–267.

54. Sugiyama, H.; Nitta, T.; Horii, M.; Motohashi, K.; Sakai, J.; Usui, T.; Hisamichi, K.; Ishiyama, J. The conformation of alpha-(1 -> 4)-linked glucose oligomers from maltose to maltoheptaose and short-chain amylose in solution. *Carbohydr. Res.* **2000**, *325*, 177–182.

55. Le Meins, J.F.; Houg, C.; Borsali, R.; Taton, D.; Gnanou, Y. Morphological changes induced by addition of polystyrene to dextran-polystyrene block copolymer solutions. *Macromol. Symp.* **2009**, *281*, 113–118.

56. Boris, D.; Rubinstein, M. A self-consistent mean field model of a starburst dendrimer: Dense core *vs*. dense shell. *Macromolecules* **1996**, *29*, 7251–7260.

57. Kuga, S. Pore size distribution analysis of gel substances by size exclusion chromatography. *J. Chromatogr. A* **1981**, *206*, 449–461.